Cascade decays of heavy leptons produced by neutrinos*

V. Barger, T. Gottschalk, and D. V. Nanopoulos
Physics Department, University of Wisconsin, Madison, Wisconsin 53706

J. Abad†
Physics Department, University of Zaragoza, Spain

R. J. N. Phillips‡
Rutherford Laboratory, Chilton, Didcot, Oxon, England

(Received 11 April 1977)

Gauge models with two heavy leptons that decay sequentially are proposed as a mechanism for fast multilepton production by neutrinos. To quantify the predictions of such models, a specific $SU(2)\times U(1)$ model is constructed and realistic calculations are made of the heavy-lepton production and decay sequence: $\nu N \to M^- X$, $M^- \to M^0 l_1^- \bar{\nu}$, $M^0 \to l_2^- l_3^+ \nu$. Good agreement with trimuon data is found, with masses 7 GeV for M^- and 2–4 GeV for M^0. The information contained in experimental distributions of multilepton events is explored. Azimuth-momentum correlations exclude a hadron-vertex origin for the extra muons in $\mu^-\mu^-\mu^+$ and in some $\mu^-\mu^+$ events. The two undetected decay neutrinos carry off missing energy equal to 35% of the visible energy on the average; this prediction can be tested with narrow-band beams. The cascade mechanism gives rise to $\mu^-\mu^-$ and $\mu^-\mu^+$ events at about five times the $\mu^-\mu^-\mu^+$ rate. The observed trimuon rate may require a mixing of μ_L^- with M_L^- comparable to the Cabibbo angle, which strains conventional universality limits. A generalized mixing scheme which circumvents these limits and allows large ν_μ-M^- coupling is presented.

I. INTRODUCTION

The existence of heavy-lepton multiplets has frequently been postulated in gauge-theory models of the weak and electromagnetic interactions. Indications that such leptons may exist include:

(i) $e\mu$ events from SPEAR[1] confirmed at DESY[2] that most plausibly come from heavy-lepton pair production and decays;

(ii) failure to detect parity violation in atomic physics,[3] which suggests the presence of a right-handed neutral heavy-lepton–electron doublet;

(iii) evidence for b-quark production,[4] which, together with the idea of quark-lepton symmetry, suggests at least one new lepton;

(iv) speculation that the decay $\mu \to e\gamma$ may occur at the 10^{-9} level; this could proceed via heavy leptons in intermediate states (e.g., Refs. 5–7);

(v) Fast trimuon and dimuon events[8,9] which lie outside the kinematical region expected for charm production.[10]

In gauge-theory models with two or more heavy leptons, sequential decays were suggested as an interesting possibility with a distinct experimental signature.[6] The neutrino trimuon events seem to have this signature, namely three fast muons originating from the neutrino vertex with nonunique dimuon and trimuon invariant masses.[8] Our objective is to quantify the predictions of such models with heavy-lepton cascade decays.

A. Gauge models

To put the discussion in perspective, we start with a concrete $SU(2)\times U(1)$ gauge model with eight leptons and eight quarks in the following doublets (unspecified states are understood to be singlets):

$$\begin{pmatrix}\nu_e\\ e^-\end{pmatrix}_L,\ \begin{pmatrix}\nu_\mu\\ \mu^-\end{pmatrix}_L,\ \begin{pmatrix}E^0\\ E^-\end{pmatrix}_L,\ \begin{pmatrix}M^0\\ M^-\end{pmatrix}_L,\ \begin{pmatrix}E^0\\ e^-\end{pmatrix}_R,\ \begin{pmatrix}M^0\\ \mu^-\end{pmatrix}_R,$$
$$\begin{pmatrix}u\\ d_C\end{pmatrix}_L,\ \begin{pmatrix}c\\ s_C\end{pmatrix}_L,\ \begin{pmatrix}t\\ b\end{pmatrix}_L,\ \begin{pmatrix}t'\\ b'\end{pmatrix}_L,\ \begin{pmatrix}u\\ b\end{pmatrix}_R,\ \begin{pmatrix}c\\ b'\end{pmatrix}_R. \tag{1.1}$$

The first two columns are the established Glashow-Iliopoulos-Maiani (GIM) structure.[11] E^- is the SPEAR heavy lepton[1,2] with neutral partner E^0. The $(E^0, e^-)_R$ doublet eliminates parity-violating terms from the electronic neutral current and hence from atomic physics.[3] The corresponding $(u,b)_R$ quark doublet explains[4] the $\bar{\nu}N$ high-y anomaly and the rising $\sigma_t(\bar{\nu}N)/\sigma_t(\nu N)$ ratio. In fact these doublets satisfactorily account for all hitherto established experimental information regarding charged and neutral currents.[12] Extending μ-e

symmetry from the GIM sector, we obtain the lepton doublets in the final column. This scheme immediately suggests the possibility of a chain of decays[6] (Fig. 1)

$$M^- \to M^0 l_1^- \bar{\nu}\,, \qquad M^0 \to l_2^- l_3^+ \nu \tag{1.2}$$

and hence neutrino trimuon events (Fig. 2), provided there is some mixing of μ_L^- and M_L^- to generate a coupling of ν_μ to M^-. In the model above the transition $M^- \to M^0$ is $V-A$ while $M^0 \to \mu^-$ is dominantly $V+A$.

Couplings of ν_μ to M^- or M^0 can be induced through the Higgs mechanism that gives the spontaneous symmetry breakdown.[6,13] The simplest Higgs mechanisms result in couplings of order m_μ/m_M relative to the $\nu_\mu \to \mu^-$ coupling that are much too small to explain the observed trimuon rate (see Sec. VI).

By whatever mechanism it arises, the $\nu_\mu \to M^-$ coupling cannot be prescribed arbitrarily because of experimental universality tests. In a conventional scheme where the (u, d_C) doublet is not further mixed, universality restricts the $\nu_\mu \to M^-$ coupling severely. In a generalized mixing scheme (Sec. VII) or in a larger gauge group these restrictions on the size of heavy-lepton production can be avoided.[14] Although our calculations are mostly phrased in terms of our SU(2) × U(1) model above, the actual results remain valid in a much wider context.

In our calculations we take the M^- mass to be 7 GeV and the M^0 mass to be either 3.5 or 2 GeV, as suggested by experimental invariant-mass distributions.

B. Cascade decay modes

The heavy-lepton cascade can involve both leptonic and hadronic decay products

$$M^- \to M^0(l_1^- \bar{\nu}) \text{ or } M^0 H_1^-\,, \qquad M^0 \to l_2^-(l_3^+ \nu) \text{ or } l_2^- H_3^+\,, \tag{1.3}$$

where H_1^- and H_3^+ are hadronic systems, as shown in Fig. 1. Our discussion assumes that these are the dominant diagrams. From this we obtain the

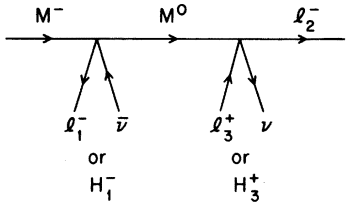

FIG. 1. Cascade decay channels.

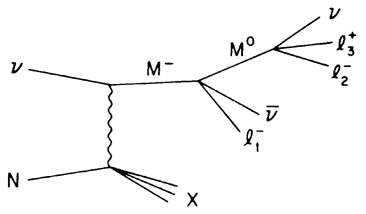

FIG. 2. Trilepton production by neutrinos via heavy-lepton cascade decay.

alternative decay categories

$$\begin{aligned} &\text{(i)}\ M^- \to l_1^- l_2^- l_3^+ \nu \bar{\nu}\,,\\ &\text{(ii)}\ M^- \to l_1^- l_2^- H_3^+ \bar{\nu}\,,\\ &\text{(iii)}\ M^- \to H_1^- l_2^- l_3^+ \nu\,,\\ &\text{(iv)}\ M^- \to H_1^- l_2^- H_3^+\,. \end{aligned} \tag{1.4}$$

For events with three charged leptons, the rates are related by

$$\begin{aligned} &N(\mu^-\mu^-\mu^+) = N(\mu^-\mu^- e^+)\,,\\ &N(e^-e^-\mu^+) = N(e^-e^-e^+)\,,\\ &N(\mu^-e^-\mu^+) = N(\mu^-e^-e^+) = N(\mu^-\mu^-\mu^+) + N(e^-e^-\mu^+) \end{aligned} \tag{1.5}$$

neglecting identical-particle interference terms. The relative rates between the different lines in Eq. (1.5) depend on the ratio of $M^0 \to \mu^-$ and $M^0 \to e^-$ couplings.

Dilepton events can arise from type (i) decays when one lepton is not identified. They also arise from (ii) and (iii), that give same-sign and opposite-sign dileptons, respectively; we expect these mechanisms to dominate over type (i). Then for the rates in the various channels we expect

$$\begin{aligned} &N(\mu^-\mu^-) \simeq N(\mu^-\mu^+) \simeq N(\mu^- e^+)\,,\\ &N(e^-e^-) \simeq N(e^-\mu^+) \simeq N(e^-e^+)\,,\\ &N(\mu^-e^-) \simeq N(\mu^-\mu^-) + N(e^-e^-)\,. \end{aligned} \tag{1.6}$$

The ratios between the different lines in Eq. (1.6) depend on the ratio of $M^0 \to \mu^-$ and $M^0 \to e^-$ couplings.

C. Trimuon rate

If we assume that e^- is unmixed, the extent of $\mu_L^- - M_L^-$ mixing is limited by the experimental check of μ-e universality

$$G_e/G_\mu = 1.007 \pm 0.014 \tag{1.7}$$

from π_{l2} decay after radiative corrections.[15] If we write the strength of the $\nu_\mu \to M^-$ charged-current coupling as ϵ relative to $\nu_\mu \to \mu^-$, then Eq. (1.7) limits ϵ by $\epsilon^2 \lesssim 0.014 \pm 0.028$. Allowing one standard deviation, we obtain

$$\epsilon^2 \lesssim 0.04\,. \tag{1.8}$$

This sets the plausible scale for ϵ, similar to the Cabibbo angle, for models where e^- is not mixed. However, this limit on ϵ can be avoided entirely in a generalized mixing scheme (Sec. VII) or in a larger gauge group.

From quark and lepton counting (neglecting charm channels which are relatively suppressed by phase space), we estimate the two branching ratios in Eq. (1.2) to be each of order 0.2. Hence asymptotically, where the ratio of M^- to μ^- production rates approaches ϵ^2, the ratio of trimuon to single-muon cross sections is approximately

$$\sigma(\mu^-\mu^-\mu^+)/\sigma(\mu^-) \simeq 2\times 10^{-3}\,, \quad E\to\infty \tag{1.9}$$

if we take $\epsilon^2 = 0.04$. At Fermilab and CERN energies, however, the M^- production cross section is substantially below its asymptotic value, and the trimuon rate is further suppressed (see Sec. II below). After averaging over the Fermilab quadrupole triplet neutrino spectrum[8] with $E_\nu > 100$ GeV we obtain

$$\sigma(\mu^-\mu^-\mu^+)/\sigma(\mu^-) \simeq 2\times 10^{-4}\,, \quad m_{M^-} = 7.0 \text{ GeV}. \tag{1.10}$$

The reported uncorrected trimuon rates are 5×10^{-4} (Ref. 8) and 1×10^{-4} (Ref. 9), based on six events and two events, respectively. If higher-statistics data indicate a substantially higher rate than Eq. (1.10), a stronger $\nu_\mu \to M^-$ coupling will be indicated; this can be achieved in a generalized mixing scheme[14] described in Sec. VII, or alternatively by adopting a larger gauge group. However, the essential dynamical features of our model calculations will still apply.

Since the incident ν_μ beam has left-handed polarization, the ν_μ-M^- coupling is necessarily $V-A$. In the model described above, the $M^-\to M^0$ and $M^0\to\mu^-$ transitions are $V-A$ and $V+A$, respectively, but for slightly greater generality we consider $V\pm A$ couplings at both of these vertices. We note this does not exhaust all possibilities: for example the existence of a $(\nu_\mu, M^-)_R$ doublet would lead to a $M^-\to\nu_\mu\mu^-\overline{M}^0$ decay with RR couplings.

D. Same-sign dimuons

The cascade-decay mechanism can also give same-sign dimuon events when the l_3^+ is an electron, or an undetected muon, or when the $l_3^+\nu$ vertex is replaced by hadrons. We approximate the detection efficiency for each muon by a multiplicative factor η, and denote the branching fraction for $M^0\to\mu^-\mu^+\nu$ by B_μ. Then the observed cross sections are

$$\begin{aligned}\sigma(\mu^-\mu^-\mu^+ \text{ observed}) &= \eta^3 B_\mu \sigma(\mu^- M^0)\,,\\ \sigma(\mu^-\mu^- \text{ observed}) &= \eta^2[(1-\eta)B_\mu + 1 - B_\mu]\sigma(\mu^- M^0)\,.\end{aligned} \tag{1.11}$$

Hence the ratio of same-sign dimuons to trimuons is

$$\sigma(\mu^-\mu^- \text{ observed})/\sigma(\mu^-\mu^-\mu^+ \text{ observed}) = (1-\eta)/\eta + (1-B_\mu)/(B_\mu\eta)\,. \tag{1.12}$$

The lower bound independent of detection efficiency is therefore

$$\sigma(\mu^-\mu^-)/\sigma(\mu^-\mu^-\mu^+) \geq (1-B_\mu)/B_\mu\,. \tag{1.13}$$

From quark counting we expect $B_\mu \approx 0.2$ and hence the $\mu^-\mu^-$ rate should be at least four times the trimuon rate. In our later Monte Carlo calculations, folding in the Fermilab quadrupole triplet ν spectrum and detection energy cuts $E_\mu > 4$ GeV, we estimate $\eta = 0.88$ for $m_- = 7$, $m_0 = 3.5$ GeV and $\eta = 0.83$ for $m_- = 7$, $m_0 = 2$ GeV. Hence we estimate the ratio

$$N(\mu^-\mu^- \text{ observed})/N(\mu^-\mu^-\mu^+ \text{ observed}) \simeq 5\,. \tag{1.14}$$

E. Opposite-sign dimuons

The cascade decay sequence also gives $\mu^-\mu^+$ events as noted in Eq. (1.6), which come dominantly through the $M^0\to\mu^-\mu^+\nu$ subchannel. These can be distinguished from $\mu^-\mu^+$ production via charmed hadrons by their different momentum-azimuth correlations (see Sec. I F below). In fact a number of the $\mu^-\mu^+$ events from the previous Harvard-Pennsylvania-Wisconsin-Fermilab (HPWF) dimuon experiment lie outside the expected charm region, providing supporting evidence for heavy-lepton production, as we discuss in Sec. V G. Another possible source of fast $\mu^-\mu^+$ pairs is direct M^0 production[16] via a neutral current arising from ν_μ-M^0 mixing.

F. Azimuth-momentum correlations

Azimuth-momentum correlations can be used to discriminate between hadronic and leptonic origins for multimuon events. Consider $\nu N\to\mu^- H$ events, with H a hadron jet: the $\mu^- H$ azimuthal angular difference about the neutrino axis is $\Delta\phi = 180°$. As the energy of a particle in the jet increases, its momentum becomes more closely correlated with the jet axis, and its azimuthal distribution relative to the μ^- becomes increasingly peaked at $\Delta\phi = 180°$. This is a crucial and distinctive property of hadron jet constituents, shared also by their decay products, e.g., muons from charm decay.[10] Section V B demonstrates that the observed trimuons do not have this property.

G. Time-reversal invariance

CP violation, or equivalently T noninvariance, can occur naturally[17] in gauge models like that of Eq. (1.1). Since the heavy-lepton-cascade mecha-

nism involves no hadronic final-state interactions, time-reversal invariance of the weak couplings implies that the following scalar triple product vanishes on average

$$\langle(\vec{p}_1+\vec{p}_2)\times\vec{p}_3\cdot\hat{p}_\nu\rangle=0\,, \tag{1.15}$$

where $\vec{p}_1$ and $\vec{p}_2$ are the μ^- momenta, $\vec{p}_3$ is the μ^+ momentum, and $\hat{p}_\nu$ is a unit vector along the beam direction. This relies on the leptonic origin alone, plus assumed CP invariance. Failure of this test would indicate substantial CP violation in the heavy-lepton sector. The five well measured events of Ref. 8 yield a value 1.8 ± 0.9 GeV^2 for this scalar product.

Each of the two terms in Eq. (1.15) can be weighted by any T-invariant function. In particular we can derive the simple geometrical prediction

$$\langle\sin(\phi_1-\phi_3)+\sin(\phi_2-\phi_3)\rangle=0 \tag{1.16}$$

for T invariance, where ϕ_i is the azimuthal angle of lepton i about the beam axis. This is satisfied by the data of Ref. 8, within two standard deviations.

H. Synopsis

In the following sections we make quantitative predictions for neutrino trimuon production and decay distributions via the cascade mechanism. Section II describes our method of calculation and presents numerical results for heavy-lepton production cross sections and the associated recoil hadron energy distributions. Section III gives the squared decay matrix elements. Section IV evaluates relations among the mean energies of heavy-lepton decay products. Section V presents calculations of the various observable distributions for the two- and three-lepton combinations. Section VI discusses a simple Higgs mechanism which generates a ν_μ-M^- coupling. Section VII describes a generalized mixing scheme that permits a large ν_μ-M^- coupling. Section VIII summarizes our conclusions.

II. PRODUCTION AND CASCADE-DECAY CALCULATION

We use a laboratory-frame helicity basis and sum over helicities of intermediate heavy leptons. An exact calculation requires coherent summation of amplitudes involving all possible combinations of intermediate helicities. Given our present incomplete knowledge of the V,A nature of the heavy-lepton couplings, the algebraic complexity of an exact evaluation is not warranted. We therefore make the simplifying approximation of neglecting interference terms between amplitudes with different intermediate helicity configurations. This retains important features of the full theory; in each amplitude the helicity is correctly followed from the production through the final stage of the decay. In any situation where a particular helicity configuration is dominant, our approximation gives the exact result. Furthermore, the neglected interference terms integrate to zero in the total rates. In any multibody process, particle masses and phase space are bound to have overriding importance in any case, and these we treat exactly.

It is convenient to distinguish the partial decay widths

$$E_-d\Gamma^{\rm I}(M_h^-\to M_j^0 l_1^-\bar{\nu})=A_{hj}^{\rm I}\prod_\alpha\frac{d^3p_\alpha}{E_\alpha}\,\delta^4\Big(p_- -\sum_\alpha p_\alpha\Big), \tag{2.1}$$

$$E_0 d\Gamma^{\rm II}(M_j^0\to l_2^- l_3^+\nu)=A_j^{\rm II}\prod_\beta\frac{d^3p_\beta}{E_\beta}\,\delta^4\Big(p_0-\sum_\beta p_\beta\Big) \tag{2.2}$$

with $\alpha=M^0,l_1,\bar{\nu}$ and $\beta=l_2,l_3,\nu$; we use $-$ and 0 subscripts to denote M^- and M^0, respectively. $A^{\rm I},A^{\rm II}$ are invariant squared matrix elements; $h,j=\pm$ are helicity labels for heavy leptons, and the helicities of l_1,l_2,l_3 (which may be either electrons or muons) have been summed over. In the approximation discussed above, the partial width for the cascade process is then

$$E_-d\Gamma^{\rm III}(M_h^-\to l_1^- l_2^- l_3^+\nu\bar{\nu})=\frac{B^{\rm II}}{m_0\Gamma^{\rm II}}\sum_j A_{hj}^{\rm I}A_j^{\rm II}\prod_\alpha\frac{d^3p_\alpha}{E_\alpha}\prod_\beta\frac{d^3p_\beta}{E_\beta}\,\delta^4\Big(p_- -\sum_\alpha p_\alpha\Big)\delta^4\Big(p_0-\sum_\beta p_\beta\Big), \tag{2.3}$$

where $\Gamma^{\rm II}$ is the partial width for $M^0\to l_1^- l_2^- l_3^+$ in the M^0 rest frame and $B^{\rm II}$ is the branching fraction for this mode.

The multilepton production cross section in our approximation is

$$d\sigma(\nu N\to l_1 l_2 l_3\nu\bar{\nu}X)=\frac{E_-B^{\rm III}}{m_-\Gamma^{\rm III}}\sum_h d\sigma_h(\nu N\to M_h^- X)d\Gamma^{\rm III}(M_h^-\to l_1 l_2 l_3\nu\bar{\nu})\,, \tag{2.4}$$

where $\Gamma^{\rm III}$ is the partial width for $M^-\to l_1^- l_2^- l_3^+\nu\bar{\nu}$ in the M^- rest frame and $B^{\rm III}$ is the branching fraction of this decay.

The M^- production by ν_μ or ν_e necessarily proceeds via $V-A$ lepton coupling, with the helicity cross sections given by

$$\frac{d\sigma^h}{dxdy}=\frac{\epsilon^2 G_F{}^2 ME}{4\pi}\left(F_1\left[y\left(xy+\frac{m_-{}^2}{2ME}\right)-h\zeta_1 y\right]\left(1+\frac{Mx}{Ey}\right)+F_2\left[2-2y-\frac{xyM}{E}-\frac{m_-{}^2}{2E^2}-h\left(2\zeta_2-\frac{M\zeta_1}{E}\right)\right]\right.$$
$$-F_3\left\{2xy-xy^2-\frac{ym_-{}^2}{2ME}-h\left[\zeta_1+\left(xy+\frac{m_-{}^2}{2ME}\right)\zeta_2\right]\right\}+F_4\left[\left(xy+\frac{m_-{}^2}{2ME}\right)+h\zeta_1\frac{m_-{}^2}{ME}\right]$$
$$\left.-F_5\left\{\frac{m_-{}^2}{ME}+h\left[\zeta_1(1-y)-\zeta_2\left(xy+\frac{m_-{}^2}{2ME}\right)\right]\right\}\right), \tag{2.5}$$

where ϵ characterizes the strength of the $\nu_\mu \to M^-$ coupling relative to $\nu_\mu \to \mu^-$, M is the nucleon mass, $x=Q^2/(2M\nu)$, $y=\nu/E$, Q and ν are the four-momentum and lab energy of the exchange current, and

$$\zeta_1=[(E_-{}^2-m_-{}^2)^{1/2}-E_-\cos\theta]/M\,,$$
$$\zeta_2=(E_-{}^2-m_-{}^2)^{1/2}/E\,. \tag{2.6}$$

In the limit of high E_- or small m_-, $\zeta_1 \to xy$, $\zeta_2 \to 1-y$, F_4 and F_5 terms in Eq. (2.5) disappear, σ_+ vanishes, and σ_- reduces to the familiar muon production cross section for $\epsilon=1$. The coefficients F_i are related to the structure functions W_i of the standard hadron tensor (with $p=p_N$ and $q=p_\nu-p_-$)

$$-W_{\mu\nu}=\delta_{\mu\nu}W_1+\frac{1}{M^2}p_\mu p_\nu W_2+\frac{1}{2M^2}\epsilon_{\mu\nu\sigma\gamma}p_\sigma q_\gamma W_3$$
$$+\frac{1}{M^2}q_\mu q_\nu W_4+\frac{1}{2M^2}(p_\mu q_\nu+q_\mu p_\nu)W_5 \tag{2.7}$$

as follows:

$$F_1=2MW_1,\quad F_i=\nu W_i \text{ for } i\neq 1\,. \tag{2.8}$$

In the quark-parton model the F_i for $\nu p \to \mu^- X$ are related to the parton densities by

$$F_1=F_2/x=F_5=2(\bar{u}+d\cos^2\theta_C+s\sin^2\theta_C)\,,$$
$$F_3=2(\bar{u}-d\cos^2\theta_C-s\sin^2\theta_C)\,, \tag{2.9}$$
$$F_4=0\,,$$

where we have neglected charm components and charm production. For $\nu n \to \mu^- X$ the u and d labels in Eq. (2.9) are interchanged. The results for $\bar{\nu}p \to \mu^+ X$ can be obtained by the following modifications: $h \to -h$ on the right-hand side of Eq. (2.5) and $u \to \bar{u}, d \to \bar{d}, s \to \bar{s}$ in Eq. (2.9). In the following calculations, we use the quark-parton distributions from solution 3 of Ref. 18.

Figure 3 shows $\nu N \to M^- X$ and $\bar{\nu}N \to M^+ X$ helicity cross sections on an isospin-averaged nucleon target N, for full-strength Fermi coupling $\epsilon=1$, with heavy-lepton masses $m_-=7$ and 3.5 GeV, compared with $\mu^\pm$ production. For neutrino beams the helicity-minus cross section dominates over helicity plus, so that the produced M^- is dominantly left-handed. Asymptotically $\sigma_+(\nu)$ and $\sigma_-(\bar{\nu})$ tend to zero, and the produced M^- (M^+) become completely left (right) polarized in this limit. Note that threshold factors suppress the cross sections appreciably, even in the 100-GeV region. The σ_M/σ_μ production cross-section ratios, averaged over the HPWF quadrupole triplet neutrino spectrum, are

	$m_-=3.5$	$m_-=7.0$
$\sigma_{M^-}/\sigma_{\mu^-}$ $(E>50)$	0.44	0.10
$\sigma_{M^-}/\sigma_{\mu^-}$ $(E>100)$	0.57	0.17
$\sigma_{M^-}/\sigma_{\mu^-}$ $(E>150)$	0.60	0.20

Figure 4 shows the distribution of hadron energy fraction $y=(E_{\rm had}-M)/E$ for various incident ν and $\bar{\nu}$ energies. The suppressed helicity component of the cross section has a very different y dependence from the dominant component. Neutrino production

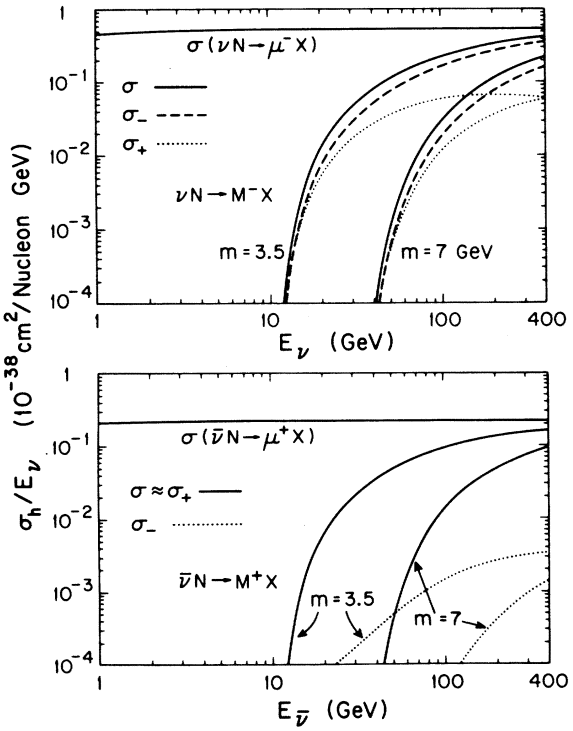

FIG. 3. Helicity cross sections for ν and $\bar{\nu}$ production of heavy leptons M assuming Fermi coupling strengths and masses 3.5 and 7.0 GeV for $M^\pm$.

at high y is suppressed by the threshold; nevertheless for $y<0.5$ the distribution is relatively flat for νN and approximately $(1-y)^2$ for $\bar{\nu}N$.

III. DECAY MATRIX ELEMENTS

The leptonic cascade decay is described by the two decay segments in Eqs. (2.1) and (2.2). In each case we have a known νl $V-A$ vertex and a vertex involving heavy leptons; for the latter we consider $V-A$ and $V+A$ possibilities. We label the four-momenta in the decay by $p_a \to p_b p_c p_d$ corresponding to $M^- \to M^0 l_1^- \bar{\nu}$ or $M^0 \to l_2^- \nu l_3^+$. The squared matrix elements A for Eqs. (2.1) or (2.2) for $V-A$ are

$$A_{hj}^{V-A}[(p_a)_h \to (p_b)_j p_c p_d]$$

$$= \frac{\delta^2 G_F{}^2}{(2\pi)^5}(p_a + h\xi_a)\cdot p_d (p_b + j\xi_b)\cdot p_c \,, \quad (3.1)$$

where δ is the $a \to bcd$ transition strength relative to $G_F/\sqrt{2}$; ξ is related to the covariant spin vector S as

$$\xi = MS = (\vec{p}E/|\vec{p}|, i|\vec{p}|) \,. \quad (3.2)$$

For $V+A$ coupling, p_c and p_d are interchanged on the right-hand side of Eq. (3.1), and the ξ terms change sign. In the case of $M^0 \to l_2^- \nu l_3^+$, Eq. (3.1) is summed over the helicity j. We note that the strength parameters δ cancel out on the right-hand side of Eq. (2.4); the dependence on the δ parameters is contained in the branching fraction $B^{\rm III}$ which for present purposes may be regarded as an arbitrary parameter.

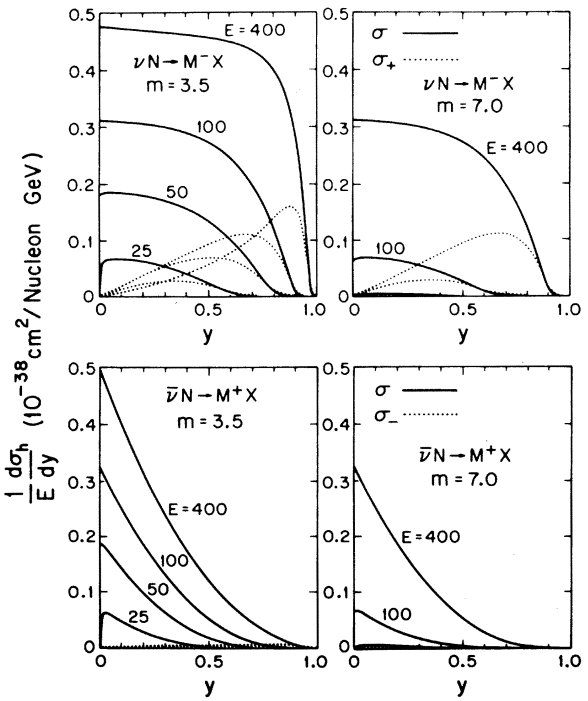

FIG. 4. Distributions of recoil-hadron energy fraction $y = (E_{\rm had} - M)/E$ associated with heavy-lepton production at neutrino energies $E = 25, 50, 100, 400$ GeV.

IV. MEAN ENERGIES OF HEAVY-LEPTON DECAY PRODUCTS

The ratios of mean energies of leptons from a heavy-lepton decay obey restrictive bounds. For arbitrary V, A couplings and initial lepton polarization, the bounds are[19]

$$\tfrac{1}{2} \le \langle E_1\rangle / \langle E_2\rangle \le 2 \quad (4.1)$$

for any two decay leptons, in the zero-mass approximation. For a specified $V \pm A$ interaction and specified heavy-lepton polarization, the average decay energies and their ratios are more restricted.

Consider the leptonic decay $a \to bc\bar{d}$ with a, b, c particles and $\bar{d}$ an antiparticle, with either $V-A$ or $V+A$ coupling at the $a \to b$ vertex (relevant for charge current decay) and $V-A$ coupling at the $c\bar{d}$ vertex. The mean decay energies are then

	$V-A$	$V+A$	
$\langle E_b\rangle/E_a =$	$(7-\vec{s}\cdot\vec{v})/20$	$(7+\vec{s}\cdot\vec{v})/20$	
$\langle E_c\rangle/E_a =$	$(7-\vec{s}\cdot\vec{v})/20$	$(6-2\vec{s}\cdot\vec{v})/20$	(4.2)
$\langle E_{\bar{d}}\rangle/E_a =$	$(6+2\vec{s}\cdot\vec{v})/20$	$(7+\vec{s}\cdot\vec{v})/20$	

in the limit of negligible $b, c, \bar{d}$ masses. Here $\vec{s}$ is the rest-frame covariant spin vector and $\vec{v}$ is the laboratory velocity of particle a.

Since $\vec{s}\cdot\vec{v}$ is always bounded by ± 1 (the limits being reached for relativistic particles), the ratios of mean energies are rigorously bounded as follows

$V-A$	$V+A$
$b/c = 1$	$\frac{3}{4} \le b/c \le 2$
$\frac{3}{4} \le b/\bar{d} \le 2$	$b/\bar{d} = 1$
$\frac{3}{4} \le c/\bar{d} \le 2$	$\frac{1}{2} \le c/\bar{d} \le \frac{4}{3}$.

(4.3)

For massive b the results corresponding to Eqs. (4.2)–(4.3) are more complicated. They take the general form

$$\langle E_i\rangle/E_a = A_i(x) - \tfrac{1}{3}B_i(x)\vec{s}\cdot\vec{v} \,, \quad (4.4)$$

where A_i and B_i are functions of $x=m_b/m_a$. For $V-A$ coupling at the $a\to b$ vertex they have the forms

$$\begin{aligned}
IA_b &= 7-25x^2+160x^4-160x^6+25x^8-7x^{10} \\
&\quad +120x^4(1+x^2)\ln x\ , \\
IB_b &= 3-15x^2+200x^4-120x^6-75x^8+7x^{10} \\
&\quad +120x^4(1+3x^2)\ln x\ , \\
IA_c &= 7-75x^2-120x^4+200x^6-15x^8+3x^{10} \\
&\quad -120x^4(3+x^2)\ln x\ , \\
IB_c &= 3-45x^2-240x^4+240x^6+45x^8-3x^{10} \\
&\quad -360x^4(1+x^2)\ln x\ , \\
IA_{\bar d} &= -IB_{\bar d} = 6-60x^2-40x^4+120x^6-30x^8 \\
&\quad +4x^{10}-240x^4\ln x\ ,
\end{aligned} \tag{4.5}$$

where

$$I=20(1-8x^2+8x^6-x^8-24x^4\ln x)\ .$$

To obtain the case of $V+A$ coupling at the $a\to b$ vertex, reverse the sign of all coefficients B_i and interchange the labels $c,\bar d$ in Eq. (4.5).

The corresponding average decay energies are plotted in Fig. 5 for $\vec s\cdot\vec v=\pm1$, for $V-A$ coupling at the $a\to b$ vertex. For $V+A$ coupling at this vertex, the $\vec s\cdot\vec v=\pm1$ labels in Fig. 5 should be reversed and $E_c, E_{\bar d}$ curves should also be interchanged.

Using Eqs. (4.2) and (4.4), plus the information that M^- is relativistic ($v\simeq1$) and dominantly left-handed ($\vec s\cdot\vec v\simeq-1$), we can deduce the decay energies for the cascade $M^-\to M^0 l_1^-\bar\nu$, $M^0\to l_2^- l_3^+\nu$. We take $V-A$, $V+A$ couplings at the $M^-\to M^0$, $M^0\to l_2^-$ vertices and masses $m_-=7$ GeV, $m_0=3.5$ or 2 GeV as before. The results expressed as a fraction of the average grandparent M^- energy are

	$m_0=3.5$ GeV	$m_0=2.0$ GeV
$\langle M^0\rangle/\langle M^-\rangle=$	0.62	0.49
$\langle l_1^-\rangle/\langle M^-\rangle=$	0.24	0.33
$\langle\bar\nu\rangle/\langle M^-\rangle=$	0.14	0.18
$\langle l_2^-\rangle/\langle M^-\rangle=$	$0.22(1+\vec s_0\cdot\vec v_0/7)$	$0.17(1+\vec s_0\cdot\vec v_0/7)$
$\langle l_3^+\rangle/\langle M^-\rangle=$	$0.22(1+\vec s_0\cdot\vec v_0/7)$	$0.17(1+\vec s_0\cdot\vec v_0/7)$
$\langle\nu\rangle/\langle M^-\rangle=$	$0.18(1-\vec s_0\cdot\vec v_0/3)$	$0.15(1-\vec s_0\cdot\vec v_0/3)$

(4.6)

where $\vec s_0, \vec v_0$ refer to M^0.

The calculated ratios of decay energies based on our approximation to the production-decay sequence, including corrections due to muon-energy acceptance cuts and right-handed M^- contributions, are in fact quite close to the idealized theoretical predictions of Eq. (4.6): see Eq. (4.7). For the Fermilab quadrupole triplet ν spectrum, $\sigma(\vec s\cdot\vec v=-1)/\sigma(\vec s\cdot\vec v=+1)\simeq3$. For high-energy M^- production, we find $\langle\vec s_0\cdot\vec v_0\rangle\simeq-0.3$ for $m_0=3.5$ GeV and $\langle\vec s_0\cdot\vec v_0\rangle\simeq-0.5$ for $m_0=2$ GeV.

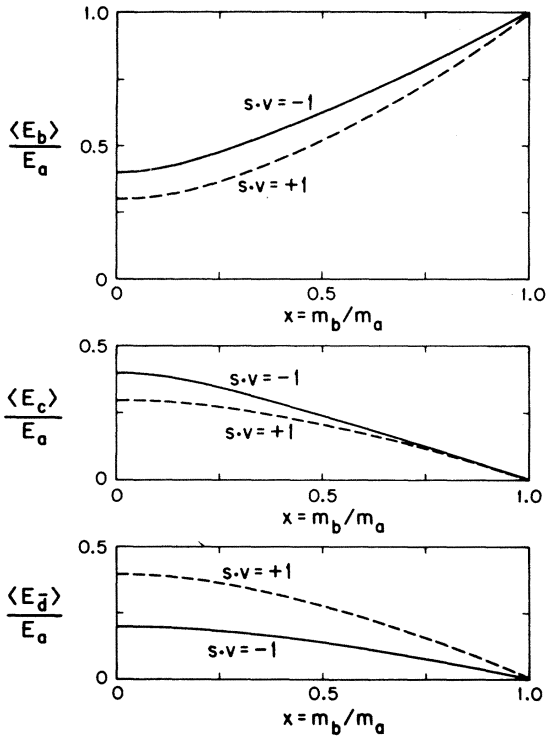

FIG. 5. Average energies of decay leptons in $a\to bc\bar d$, relative to the parent energy, as a function of the mass ratio $x=m_b/m_a$. Here $c,\bar d$ are massless and $V-A$ coupling at both $a\to b$ and $c\to d$ vertices is assumed. The curves represent upper and lower bounds corresponding to $\vec s\cdot\vec v=\pm1$. For $V+A$ coupling at the $a\to b$ vertex, interchange the $\vec s\cdot\vec v=\pm1$ cases and exchange the $c,\bar d$ labels.

The actual mean decay energies from the model calculation with the experimental ν_μ spectrum and acceptance cuts $E_\mu>4$ GeV are as follows in GeV units:

	$m_0=3.5$	$m_0=2.0$
$\langle M^-\rangle=$	126	129
$\langle M^0\rangle=$	75	63
$\langle l_1^-\rangle=$	30	40
$\langle\bar\nu\rangle=$	20	26
$\langle l_2^-\rangle=$	25	21
$\langle l_3^+\rangle=$	26	21
$\langle\nu\rangle=$	24	21

(4.7)

It is impossible to know experimentally which of the two negative leptons is l_1^- and which is l_2^-; these two leptons can be classed as fast and slow, which does not identify the vertices of origin. As M^0 becomes lighter, l_1 tends to become the faster lepton on average. With the fast-slow classifications, our calculation gives mean energies (in GeV)

	$m_-=7.0$ $m_0=3.5$	$m_-=7.0$ $m_0=2.0$	$m_-=10.0$ $m_0=2.0$
$\langle l_F^- \rangle =$	39	45	53
$\langle l_S^- \rangle =$	17	15	23

(4.8)

where we include one example with higher m_- for comparison. Three other quantities of interest are the hadron energy $E_{\rm had}$, the total visible energy $E_{\rm vis}$, and the total energy; for $m_-=7.0$ we find the mean values (in GeV)

	$m_0=3.5$	$m_0=2.0$
$\langle E_{\rm had} \rangle =$	49	47
$\langle E_{\rm vis} \rangle =$	131	129
$\langle E_{\rm total} \rangle =$	175	175.

(4.9)

The mean missing energy carried by neutrinos is about 55% of the 3μ energy and about 35% of the total visible energy. The incident neutrino energy is appreciably higher than the visible energy; this prediction can be tested with narrow-band beams.

The experimental results of Ref. 8 give (in GeV)

$$\begin{aligned} &\langle \mu_F^- \rangle = 59 \pm 5 , \\ &\langle \mu_S^- \rangle = 13 \pm 2 , \\ &\langle \mu^+ \rangle = 31 \pm 6 , \\ &\langle E_{\rm had} \rangle = 52 \pm 5 , \\ &\langle E_{\rm vis} \rangle = 183 \pm 11 , \end{aligned} \tag{4.10}$$

where the errors quoted are measurement errors only. The number of events in these average values are 6, 6, 5, 3, 3, respectively. These energy averages are in the neighborhood of our predictions.

V. COMPARISON WITH EXPERIMENTAL DISTRIBUTIONS

A. Invariant-mass distributions

The invariant-mass distribution for the $l_2^- l_3^+$ leptons from M^0 decay has been calculated previously.[20] Defining $s=(m_{23})^2$, the result is

$$\begin{aligned} \frac{1}{\Gamma^{\rm II}} \frac{d\Gamma^{\rm II}}{ds} &= 2(m_0^2 - s)^2(m_0^2 + 2s)/m_0^8 \quad (V-A) \\ &= 12s(m_0^2 - s)^2/m_0^8 \quad (V+A) . \end{aligned} \tag{5.1}$$

This distribution is interesting for opposite-sign dileptons originating in M^- cascade decay, since there $l^- l^+$ come dominantly from M^0. The average values from Eq. (5.1) are

$$\begin{aligned} \langle m_{23} \rangle &= \frac{32}{63} m_0 \quad (V-A) \\ &= \frac{64}{105} m_0 \quad (V+A) . \end{aligned} \tag{5.2}$$

For the cascade decay $M^- \to l_1^- l_2^- l_3^+ \nu \bar{\nu}$ we make Monte Carlo calculations based on Eqs. (2.3) and (3.1) for the observable invariant-mass combinations $m_{--+} = m(l_1^- l_2^- l_3^+)$, $m_{--} = m(l_1^- l_2^-)$, and $m_{-+} = m(l_1^- l_3^+)$ or $m(l_2^- l_3^+)$, summing the latter indistinguishable alternatives. Figure 6 shows the results for the four possible $V \pm A$ coupling possibilities at the heavy-lepton vertices, with masses $m_- = 7$ GeV and $m_0 = 3.5$ GeV. The similarity of the invariant-mass distributions for different coupling choices supports our expectation that phase space would be a dominant effect. The $V-A, V-A$ case has also been calculated independently in a different approximation, with similar results.[21]

The kinematical end-point of all three invariant-mass distributions above is the mass of the M^- parent. The m_{--+} distribution most clearly reflects this scale, with $\langle m_{--+} \rangle \simeq \frac{1}{2} m_-$. The lower peaking of m_{-+} is partly due to the M^0 component, which from Eq. (5.2) has $\langle m_{-+} \rangle \simeq \frac{1}{2} m_0$.

Figure 7 compares the LR choice, corresponding to the model of Eq. (1.1), with the HPWF trimuon data. Here two choices $m_0 = 3.5$ and $m_0 = 2$ GeV are shown, with $m_- = 7$ GeV. The previous invariant-mass distributions are somewhat insensitive to the precise value of m_0. However, in each event the lower of the two m_{-+} combinations must always be less than m_0: in Fig. 8 we show the distributions of m_{-+}(lower), for which the kinematical end point is m_0. The data exclude $m_0 < 2$ GeV; the event at the high end of the distribution has m_{-+}(lower) $= 2.2 \pm 0.2$ GeV.

B. Azimuth-momentum correlations

As remarked in the Introduction, azimuth-momentum correlations provide a means of distinguishing between heavy-lepton and hadron origins for multilepton production by neutrinos. Energetic particles from the hadron vertex tend to come out with $\Delta\phi \simeq 180°$ relative to the fast μ^- from the ν_μ vertex. Figure 9 illustrates this for dimuons from charm decay ($\nu_\mu N \to \mu^- DX, D \to K^* \mu^+ \nu$). This figure also shows a similar

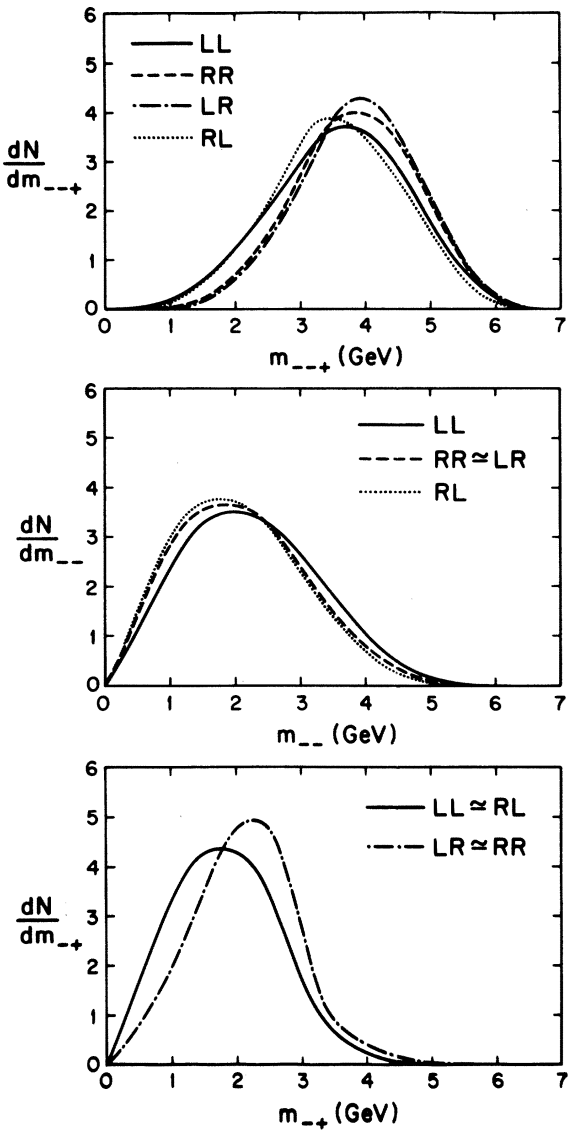

FIG. 6. Invariant-mass distributions for trimuon events of cascade decay origin. The L and R labels denote the $M^- \to M^0$ and $M^0 \to l_2^-$ couplings, in that order. The M^- and M^0 masses are taken to be 7.0 and 3.5 GeV, respectively. Units of N are arbitrary.

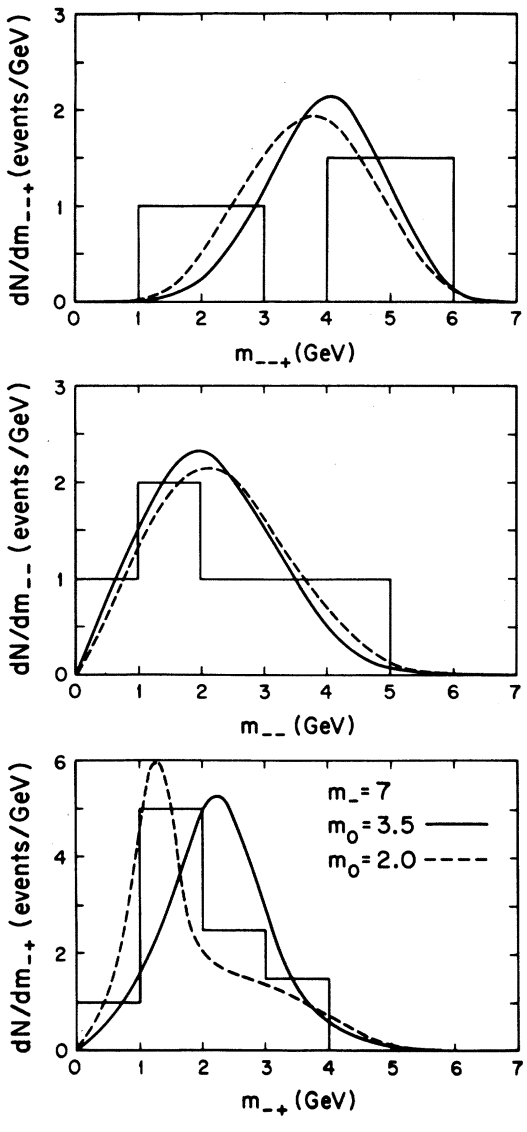

FIG. 7. Invariant-mass distributions for trimuon events with the LR coupling choice of our model. Two choices $m_0 = 3.5$ and $m_0 = 2$ GeV are shown, with $m_- = 7$ GeV. The trimuon data in this and succeeding figures are from Ref. 8.

azimuth-momentum correlation plot for the trimuon data[8]: here $\Delta\phi$ is computed between the fast μ^-, assumed to come from the ν_μ vertex, and either of the other muons. If the two slow muons came from decaying hadrons, the correlation plot should be similar to the charm case, but it is clearly not. The corresponding azimuth-momentum correlation for trimuons predicted by our heavy-lepton-cascade model is also shown in Fig. 9: there is no strong $\Delta\phi$ dependence here, in agreement with the data.

C. Muon rapidity distributions

The rapidity variable $y = \frac{1}{2}\ln[(E+p_z)/(E-p_z)]$ has proved to be extremely useful in analyzing secondary-particle distributions and correlations in multiparticle hadron physics. We expect that it will also prove useful in studying high-energy neutrino phenomena. If we neglect corrections of order $m^2/(p^2\theta^2)$, which is generally a very good approximation for muons, rapidity reduces to a purely angular variable, $y = \ln\cot(\frac{1}{2}\theta)$.

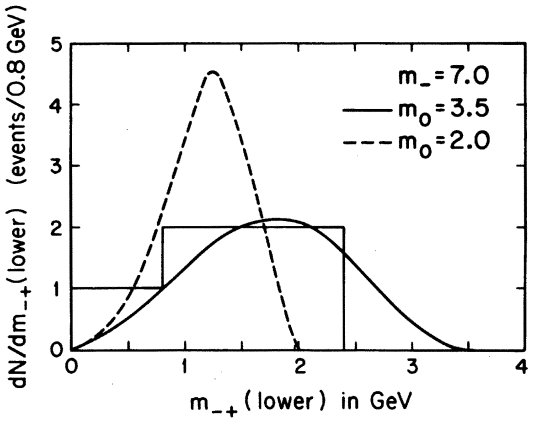

FIG. 8. Distribution of the lower of the two $\mu^-\mu^+$ invariant masses in each event, for which the kinematical end-point is m_0.

Predicted rapidity distributions are compared with results from trimuon events in Fig. 10. Individual muon rapidities are large but rapidity differences are small, in complete accord with the heavy-lepton predictions.

D. Energy distributions

Figure 11 shows the predicted energy distributions for leptons originating in the two stages of M^- decay, integrating over the ν production spectrum and including $E_\mu > 4$ GeV cuts. Figure 12 compares the predicted μ_F^-, μ_S^-, μ^+ energy distributions with histograms of the data. The agreement is broadly satisfactory. One event has $E(\mu_F^-) = 157 \pm 24$ GeV which is on the tail of the predicted spectrum. It is interesting to speculate that such an event might have originated in a single-step neutral-current decay $M^- \to \mu^-\mu^-\mu^+$: if so, future accumulations of trimuon events should occur with unique invariant mass m_{--+} as well as higher muon and visible energies than cascade decay events.

Figure 13 shows distributions for $E(M^-)$, E(hadrons), E(visible), and E(missing) with ν spectrum average and muon cuts.

E. Transverse-momentum distributions

The transverse momenta p_t of decay products provide another means of determining the mass of the parent when the p_t distributions of the parent

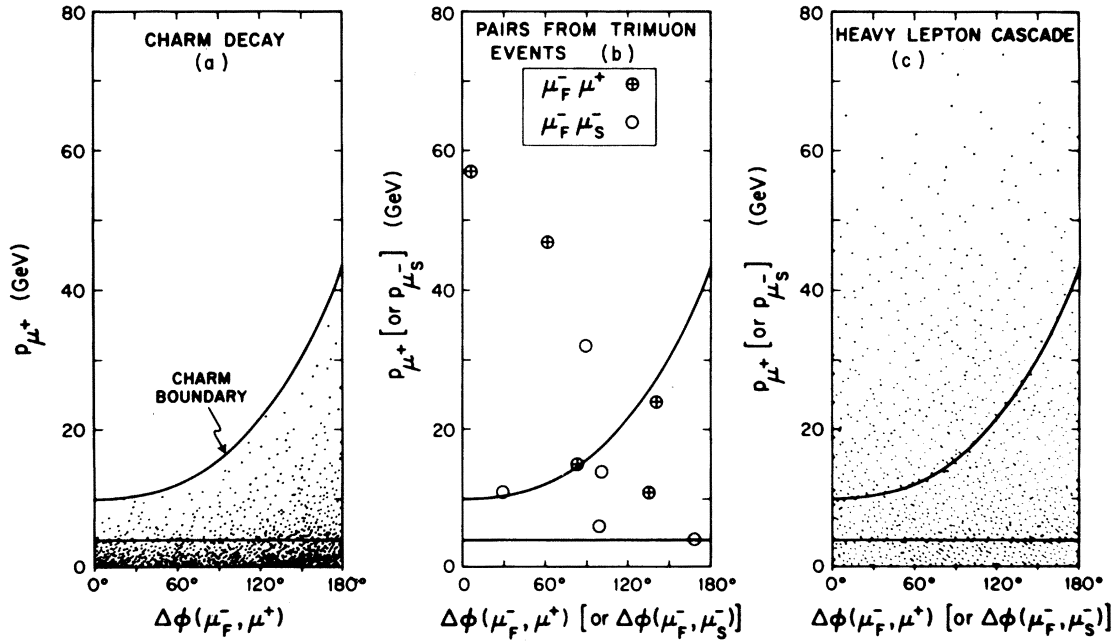

FIG. 9. Momentum-azimuth correlation test of hadronic versus leptonic origin for multimuon events. (a) Momentum of the slow μ^+ versus its azimuthal separation from the fast μ-, calculated for dimuons from charm production, $\nu N \to \mu^- DX$, $D \to K^* \mu^+ \nu$. (c) Momentum of slow cascade decay products of heavy leptons (μ^+ or μ_S^-) versus their azimuthal separations from the faster negative muon (μ_F^-). The Monte Carlo theoretical distributions are normalized to 1000 events in each case. (b) The trimuon data are shown for comparison, with the momentum of each slow muon (μ_S^- or μ^+) plotted versus its azimuthal separation from μ_F^-. The solid curve indicates a very conservative empirical boundary of the charm region and the line at $p_\mu = 4$ denotes the experimental acceptance cut.

is known. This method has previously been successfully exploited in deducing the mass of charmed mesons produced by neutrinos.[20,22] The technique should be more reliable in heavy-lepton mass determinations, since the p_t distribution of the produced M^- lepton is specified by an established theory and the identities of the decay products can be surmised.

Figure 14 compares predicted p_t distributions for μ^- (summed over both) and μ^+ with histograms from the trimuon events. If M^- were produced with zero transverse momentum, the decay muon p_t distributions would be bounded by $\frac{1}{2}m_-$: The curves show that the M^- production process smears the p_t distributions very little beyond this value. The experimental p_t distributions indicate an M^- mass about 7 GeV.

F. Angular correlations

Figure 15 shows the distributions in the opening angles between μ_F^-, μ_S^-, μ^+, taken in pairs, for trimuon events. A scatter plot of Monte Carlo events in Fig. 16 shows the correlation between the $\mu^+\mu_F^-$ and $\mu^+\mu_S^-$ opening angles; our model predicts a tendency for the $\mu^+\mu_F^-$ angle to be the smaller of the two, which is also seen in the data.

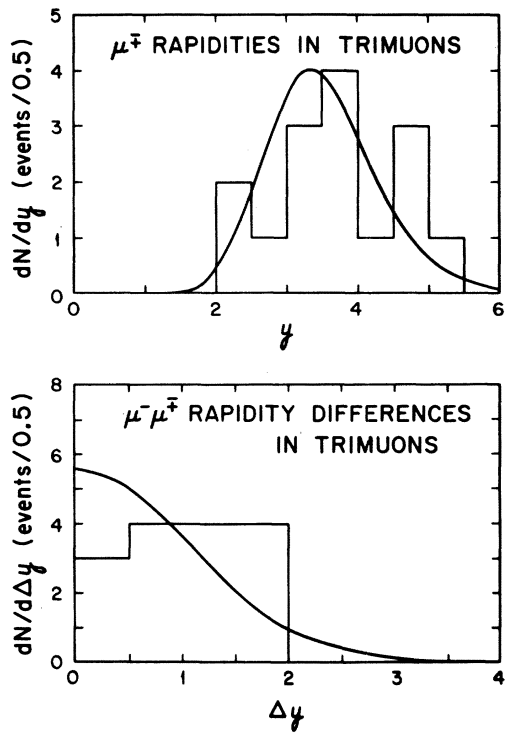

FIG. 10. Rapidity distributions of muons from heavy-lepton cascade decays, for the ν spectrum of Ref. 8 with energy acceptance cuts $E_\mu > 4$ GeV. The $y^\pm$ distributions for $\mu^\pm$ have similar forms and are shown combined. The rapidity differences Δy^{-+} and Δy^{--} also resemble one another and are shown combined. The histograms are trimuon data.

G. Dimuons

The present multimuon event rates have approximate ratios[8,9,23,24]

$$\mu^-:\mu^-\mu^+:\mu^-\mu^-:\mu^-\mu^-\mu^+ \simeq 1:10^{-2}:1.5\times10^{-3}:(0.1\text{–}0.5)\times10^{-3}\,. \quad (5.3)$$

The $\mu^-\mu^-$ to $\mu^-\mu^-\mu^+$ ratio is consistent with the lepton cascade prediction in Eq. (1.14). From the prediction of Eq. (1.6) that $\mu^-\mu^+ \simeq \mu^-\mu^-$ for a lepton of cascade origin, we are led to expect that about 15% of the observed $\mu^-\mu^+$ events are due to M^- production and decay.

To obtain dimuon distributions of heavy-lepton cascade origin we approximate the hadronic vertex by light quarks; the calculation then reduces to the trimuon analysis. Figures 17 and 18 show azimuth-momentum correlation plots, similar to those used to discriminate against hadronic origin in Sec. V B above, applied to the dimuon events. A significant fraction of the $\mu^-\mu^+$ events from Ref. 23 lie above the boundary for charm production by neutrinos. A few of the $\mu^-\mu^+$ events, with $p(\mu^+) > p(\mu^-)$, have in the past been identified as due to charm production by antineutrinos (these events are circled in Fig. 17); however, they may as well be due to heavy leptons. Even excluding these circled events, there remain some $\mu^-\mu^+$ events outside the expected charm region.

VI. HIGGS-MECHANISM-INDUCED NEUTRINO-LEPTON COUPLINGS

We discuss briefly a Higgs mechanism which generates a coupling between ν_μ and M^-. Working within the muon sector of Eq. (1.1), we use three doublets and one singlet of leptons

$$d_L=\begin{pmatrix}\nu_\mu\\ \mu^-\end{pmatrix}_L,\quad D_L=\begin{pmatrix}M^0\\ M^-\end{pmatrix}_L,\quad D_R=\begin{pmatrix}M^0\\ \mu^-\end{pmatrix}_R,\quad S_R=M_R^-, \quad (6.1)$$

together with a Higgs doublet

$$\phi_D=\begin{pmatrix}\phi^+\\ \phi^0\end{pmatrix}$$

and one Higgs singlet ϕ'. The interaction Lagrangian density is

$$\mathcal{L}_I=-h_1\bar{d}_L D_R\phi'-h_2\bar{D}_L D_R\phi'-h_3\bar{D}_L\phi_D S_R+\text{H.c.} \quad (6.2)$$

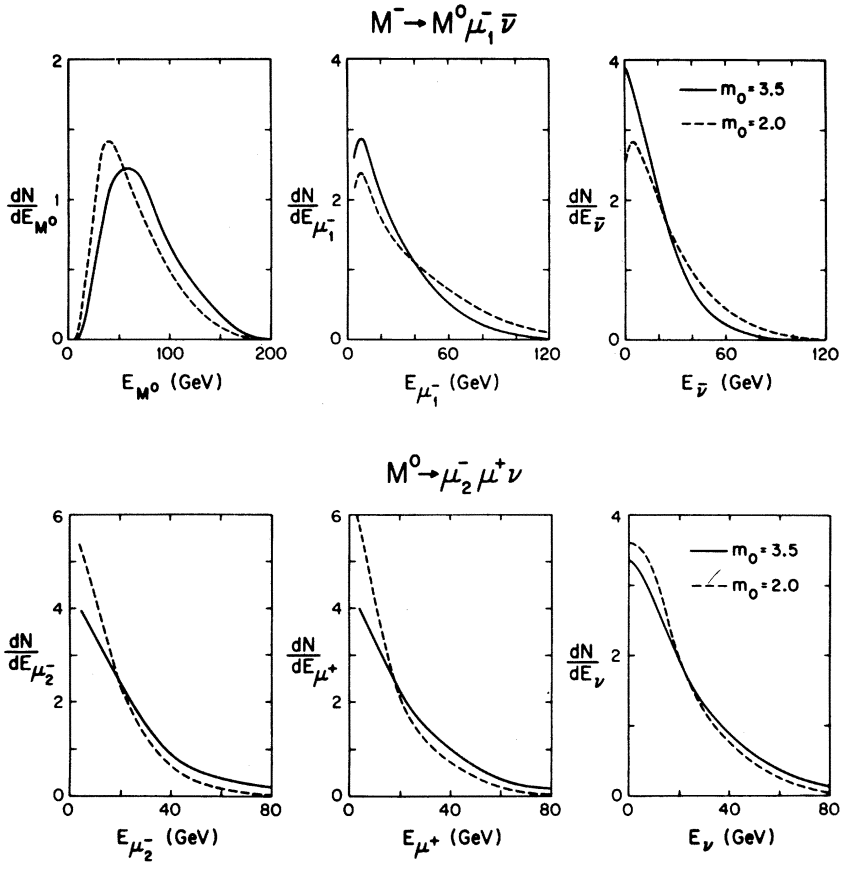

FIG. 11. Predicted energy distributions for decay products from the two stages of the cascade decay, $M^- \to M^0 \mu_1^- \bar{\nu}$, $M^0 \to \mu_2^- \mu^+ \nu$, for the quadrupole triplet ν spectrum with $E_\mu > 4$ GeV acceptance cuts. The two cases $m_0 = 3.5$ GeV and $m_0 = 2$ GeV are shown. Units of N are arbitrary.

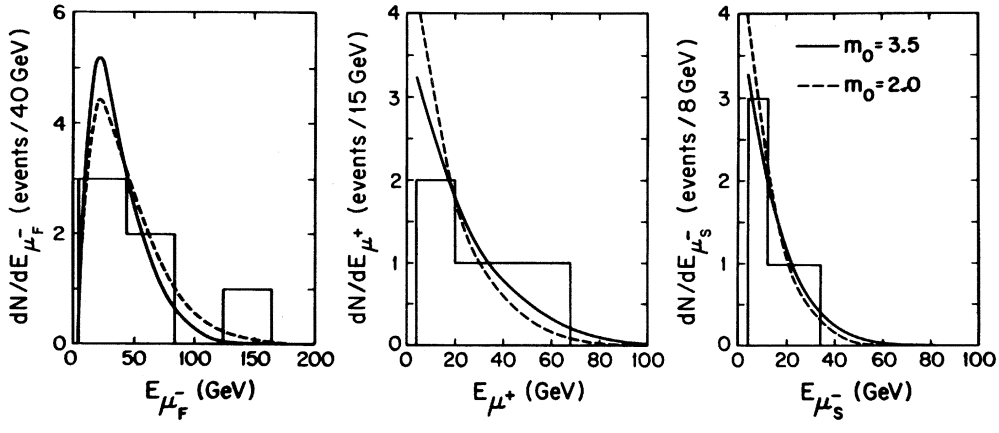

FIG. 12. Energy distributions for μ_F^-, μ_S^-, μ^+ from M^- decay compared with histograms from trimuon events.

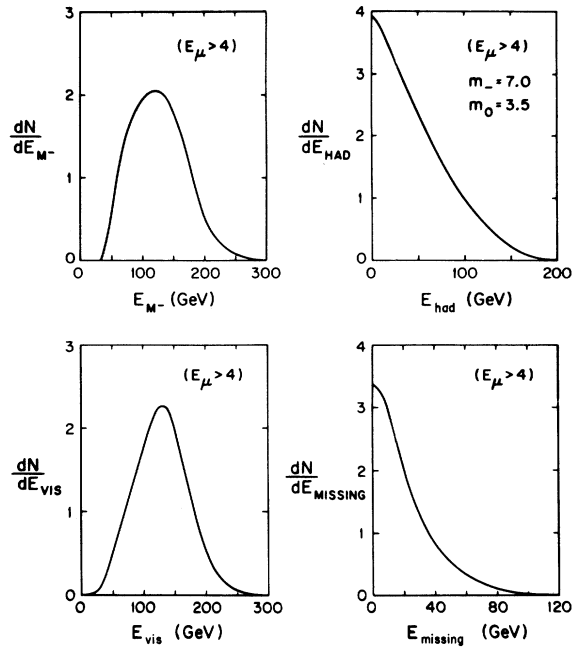

FIG. 13. Predicted distributions of M^- energy, hadron energy, visible energy, and missing energy, averaged over the ν spectrum with muon energy cuts. Units of N are arbitrary.

The Higgs fields have vacuum expectation values $\langle\phi^+\rangle=0$, $\langle\phi^0\rangle=v$, $\langle\phi'\rangle=v'$, so that the mass operator for lepton fields is essentially

$$M=a_1\bar{d}_L D_R+a_2\bar{D}_L D_R+a_3\bar{M}^-_L M^-_R+\text{H.c.}\,, \qquad (6.3)$$

where $a_1=h_1v'$, $a_2=h_2v'$, $a_3=h_3v$. Alternatively, the first two terms in Eq. (6.3) can be introduced as gauge-invariant bare mass terms. The mass operator can be diagonalized by the transformations

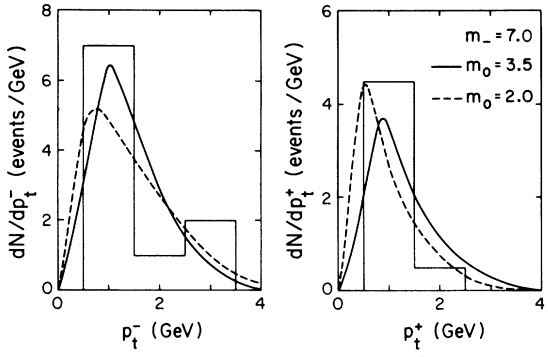

FIG. 14. Predicted transverse-momentum distributions, relative to the ν-beam axis, with neutrino spectrum average and muon energy cuts. The histograms are from trimuon events.

$$\begin{aligned}
&\nu_L \to \nu_L\cos\alpha + M^0_L\sin\alpha\,,\\
&M^0_L \to M^0_L\cos\alpha - \nu_L\sin\alpha\,,\\
&\mu^-_L \to \mu^-_L\cos\beta + M^-_L\sin\beta\,,\\
&M^-_L \to M^-_L\cos\beta - \mu^-_L\sin\beta\,,\\
&\mu^-_R \to \mu^-_R\cos\gamma + M^-_R\sin\gamma\,,\\
&M^-_R \to M^-_R\cos\gamma - \mu^-_R\sin\gamma\,,
\end{aligned} \qquad (6.4)$$

where

$$\begin{aligned}
&\tan\alpha = a_1/a_2\\
&\tan2\beta = 2a_1a_2/(a_3^2+a_2^2-a_1^2)\,,\\
&\tan2\gamma = 2a_2a_3/(a_3^2-a_2^2-a_1^2)\,,\\
&m_\mu = a_3\sin\beta/\sin\gamma\,,\\
&m_0 = (a_1^2+a_2^2)^{1/2}\,,\\
&m_- = a_1\sin\gamma/\sin\beta\,.
\end{aligned} \qquad (6.5)$$

Equation (6.5) has a simple approximate solution

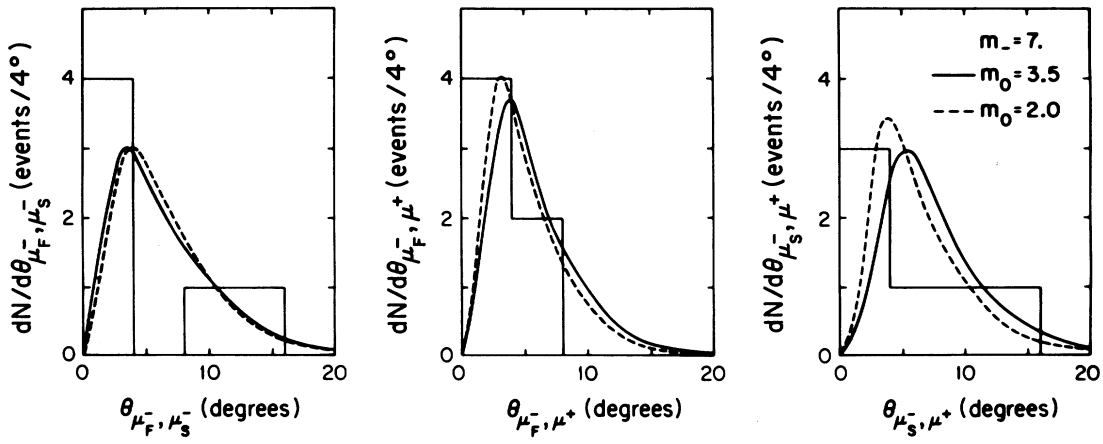

FIG. 15. Predicted distributions of opening angles between pairs of muons from M^- decay, spectrum-averaged with muon energy cuts, compared with histograms of trimuon data.

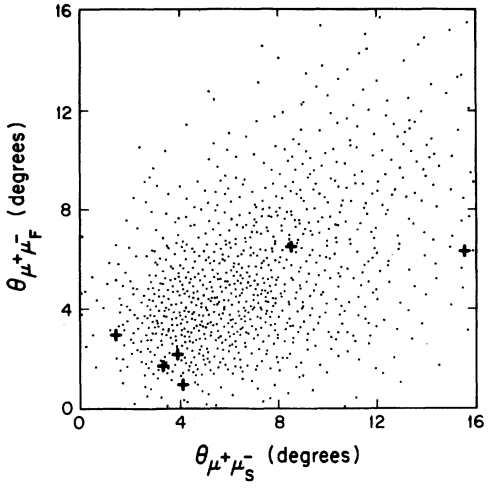

FIG. 16. Scatter plot showing the predicted correlation between $\mu_F^-\mu^+$ and $\mu_S^-\mu^+$ opening angles in M^- cascade decay, with ν spectrum average and muon energy cuts. Trimuon events are shown as crosses.

in the limit where $m_\mu \ll m_0 \ll m_-$, namely

$$a_1 = m_\mu,\ a_2 = m_0,\ a_3 = m_-,$$
$$\alpha = m_\mu/m_0,\ \beta = m_\mu m_0/m_-^2,\ \gamma = m_0/m_- . \tag{6.6}$$

With the masses $m_\mu = 0.106$, $m_0 = 3.5$, $m_- = 7.0$ GeV, the exact numerical solution of Eq. (6.5) gives

$$\alpha = 0.035,\ \beta = 0.009,\ \gamma = 0.523 . \tag{6.7}$$

This Higgs mechanism generates a $\nu_\mu - M^-$ coupling of strength $\epsilon = \tan(\beta - \alpha)$ relative to the $\nu_\mu - \mu^-$ coupling. For the numerical solution in Eq. (6.7),

$$\epsilon^2 = 0.7 \times 10^{-3} \tag{6.8}$$

which is much smaller than the minimum value $\epsilon^2 = 0.4$ needed to explain the trimuon data.

VII. UNIVERSALITY AND NEW LEPTON MIXING

A. Generalized weak universality

The constraint $\epsilon^2 \lesssim 0.04$ of Eq. (1.8) was based on the usual tacit assumption that mixings in the e, μ, and quark sectors are uncorrelated. However, weak universality constraints actually admit a hitherto unexploited maximal mixing of electrons and muons with charged heavy leptons,[14,25] which in turn allows heavy-lepton production by ν_μ with full Fermi coupling strength.

In SU(2) × U(1) gauge models the charged-current interaction Lagrangian is constructed from quark and lepton doublets D_L, D'_R as

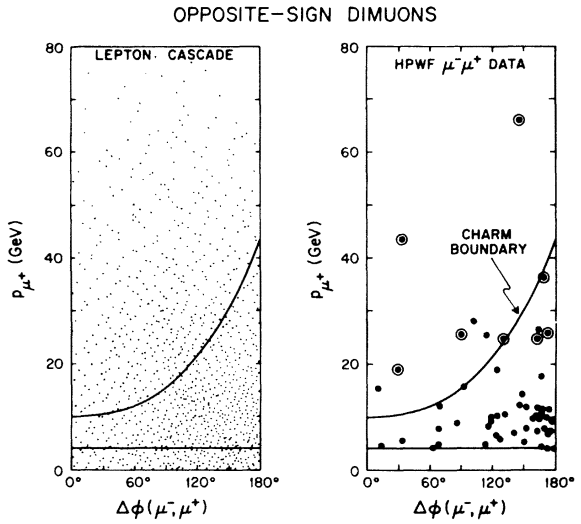

FIG. 17. Momentum-azimuth correlation plot for $\mu^-\mu^+$ events, analogous to Fig. 9 for trimuons. The solid curve is a conservative boundary for neutrino charm production, and the line at $p_\mu = 4$ denotes the experimental acceptance cut. The theoretical scatter plot for the heavy-lepton cascade process is normalized to 1000 events. The data are from Ref. 23: points with $p(\mu^+) > p(\mu^-)$ that have in the past been interpreted as antineutrino charm production are circled.

$$\mathcal{L}_I = 2m_W(G'/\sqrt{2})^{1/2} \sum_{D,D'} (\bar{D}_L \gamma_\mu \tau^+ D_L + \bar{D}'_R \gamma_\mu \tau^+ D'_R) W^+ + \text{H.c.}, \tag{7.1}$$

where L, R subscripts denote left, right handed-

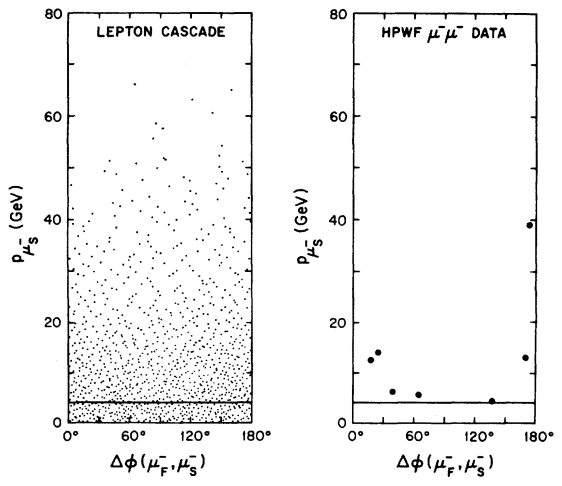

FIG. 18. Momentum-azimuth correlation plot for $\mu^-\mu^-$ events. The theoretical scatter plot for the heavy-lepton cascade process is based on 1000 events. The data are from Ref. 23.

ness. Universality of couplings requires that all doublets appearing in (7.1) are normalized to the same strength. Muon-electron universality is maintained so long as μ, e (and ν_μ, ν_e) appear symmetrically in the doublets.

The standard model[11] has $G' = G_F$, $D'_R = 0$, and the left-handed doublets of the first two columns in Eq. (1.1). For massless ν_e, ν_μ the Cabibbo rotation is the only degree of freedom with these doublets and its value is determined by experiment. The universality prediction for this model is equality of $\bar{\nu}_e e$, $\bar{\nu}_\mu \mu$, $\bar{u} d_C$ vector coupling strengths

$$g^2(\bar{\nu}_e e) : g^2(\bar{\nu}_\mu \mu) : g^2(\bar{u}d) : g^2(\bar{u}s) = 1 : 1 : \cos^2\theta_C : \sin^2\theta_C \tag{7.2}$$

which is consistent with experiment, and must be regarded as a constraint on all models.

When additional doublets exist, other rotational degrees of freedom become possible. We consider the eight left-handed doublets of Eq. (1.1) and mix them together as follows:

$$\begin{pmatrix} \nu_e \\ e^- \cos\omega + E^- \sin\omega \end{pmatrix}_L, \quad \begin{pmatrix} \nu_\mu \\ \mu^- \cos\omega + M^- \sin\omega \end{pmatrix}_L, \quad \begin{pmatrix} u\cos\omega - t\sin\omega \\ d_C \end{pmatrix}_L, \quad \begin{pmatrix} c\cos\omega - t'\sin\omega \\ s_C \end{pmatrix}_L,$$
$$\begin{pmatrix} E^0 \\ E^- \cos\omega - e^- \sin\omega \end{pmatrix}_L, \quad \begin{pmatrix} M^0 \\ M^- \cos\omega - \mu^- \sin\omega \end{pmatrix}_L, \quad \begin{pmatrix} t\cos\omega + u\sin\omega \\ b \end{pmatrix}_L, \quad \begin{pmatrix} t'\cos\omega + c\sin\omega \\ b' \end{pmatrix}_L . \tag{7.3}$$

By demanding the same mixing angle ω for each pair of doublets, we preserve e, μ symmetry, quark-lepton symmetry, plus the standard Cabibbo mixing and the constraint of Eq. (7.2) In this extended model, the coupling G' of Eq. (7.1) is

$$G' = G_F/(\cos\omega)^2 \tag{7.4}$$

to reproduce the strength of known charged-current transitions. Normalizing to G_F units, the modified left-handed weak current is

$$\begin{aligned} \tfrac{1}{2} J_\alpha = {} & \bar{\nu}_{eL}\gamma_\alpha(e^- + \tan\omega E^-)_L + \bar{\nu}_{\mu L}\gamma_\alpha(\mu^- + \tan\omega M^-)_L \\ & + \bar{E}^0_L\gamma_\alpha(E^- - \tan\omega e^-)_L + \bar{M}^0_L\gamma_\alpha(M^- - \tan\omega\mu^-)_L \\ & + \bar{u}_L\gamma_\alpha(d_C + \tan\omega b)_L + \bar{c}_L\gamma_\alpha(s_C + \tan\omega b')_L \\ & + \bar{t}_L\gamma_\alpha(b - \tan\omega d_C)_L + \bar{t}'_L\gamma_\alpha(b' - \tan\omega s_C)_L . \end{aligned} \tag{7.5}$$

Conventional models with universality have implicitly assumed $G' = G_F$, excluding anything other than Cabibbo mixing in the standard sector of Eq. (2). Only by this new mixing can we achieve a substantial coupling of ordinary neutrinos to heavy leptons M^-, or left-handed coupling of u to b, without violating the constraint Eq. (7.2).

There may also be mixing in the right-handed sector, e.g.,

$$\begin{pmatrix} E^0 \\ e^- \cos\gamma + E^- \sin\gamma \end{pmatrix}_R, \quad \begin{pmatrix} -u\cos\gamma + t\sin\gamma \\ b \end{pmatrix}_R,$$
$$\begin{pmatrix} M^0 \\ \mu^- \cos\gamma + M^- \sin\gamma \end{pmatrix}_R, \quad \begin{pmatrix} -c\cos\gamma + t'\sin\gamma \\ b' \end{pmatrix}_R, \tag{7.6}$$

where the mixing angles are equal for quark-lepton symmetry, but may be different from those in the left-handed sector. The γ mixing cannot be large, because it permits the neutral-current decays $M^- \to \mu^- l^+ l^-$ and $E^- \to e^- l^+ l^-$, which are known not to be the major decay models of M^- and E^-. To be consistent with the experimental upper limit[26]

$$\Gamma(E^- \to 3 \text{ charged leptons})/\Gamma(E^- \to \text{all}) < 0.006$$

we must require[27] $\tan^2\gamma < 0.05$. There is no compelling reason for having a nonzero γ in any case.

B. Heavy-lepton production rate

In our ω-mixing scheme the $\nu_\mu \to M^-$ coupling strength is $\tan\omega$ relative to $\nu_\mu \to \mu^-$. This allows for M^- production by neutrinos at high energy, with asymptotic ratio

$$\sigma(\nu_\mu N \to M^- X)/\sigma(\nu_\mu N \to \mu^- X) = \tan^2\omega . \tag{7.7}$$

To the extent that the coupling $\epsilon = 0.2$ in Eq. (1.8) is not in disagreement with present experimental information on the trimuon rate [see Eq. (1.10)], the rotation angle ω is approximately of the same magnitude as the Cabibbo angle.

C. W-boson mass

In a unified theory[28] based on the doublets in Eq. (7.3), the $W^\pm$ mass is

$$m_W = (37.7 \text{ GeV}) \times (\cos\omega/\sin\theta_W) \tag{7.8}$$

where θ_W is the Weinberg angle.

D. Z^0-boson mass and neutral currents

The ω rotation in Eq. (7.3) drops out of the neutral current, except insofar as it appears in the overall strength G'/κ^2, where $\kappa = m_Z \cos\theta_W/m_W$, Z being the neutral weak boson. The experimental determinations of θ_W from ratios of neutral-current

cross sections are thus unaffected by ω.

The theoretical value of κ is fixed by the Higgs mechanism; in the Weinberg-Salam model $\kappa = 1$. The ratio of inclusive neutrino neutral-current to charge-current cross sections gives[12]

$$(G'/\kappa^2)/G_F \simeq 1 \ , \tag{7.9}$$

within 10%, which implies the usual result

$$m_Z \simeq 2(37.7 \text{ GeV})/\sin(2\theta_W) \simeq 78 \text{ GeV} \ . \tag{7.10}$$

E. Muon anomalous magnetic moment

In our model the major weak contribution to $a_\mu = \frac{1}{2}(g_\mu - 2)$ comes from the triangle diagram with intermediate M^0, which gives

$$a_\mu(M^0) = \frac{G_F m_\mu^2}{\sqrt{2}\,\pi^2}\left[-g_L g_R \frac{m_0}{m_\mu} + \frac{5}{12}(g_L^2 + g_R^2)\right], \tag{7.11}$$

where $g_L = -\tan\omega$, $g_R = \cos\gamma/\cos\omega$, and m_0 is the mass of M^0. Taking $\cos\gamma \simeq 1$ and adding the contribution of the intermediate-neutrino diagram,[29] which has $g_L = 1$, $g_R = 0$, $m_0 = 0$, we obtain

$$a_\mu(M^0) + a_\mu(\nu) = 9.2 \times 10^{-9}\left(\frac{m_0}{m_\mu}\sin\omega + \frac{5}{6}\right)/\cos^2\omega \ . \tag{7.12}$$

The Z^0-exchange contribution is negligible, of order 10^{-10}. The trimuon analysis indicates $m_0 \simeq 2$–3.5 GeV and $|\tan\omega| \simeq 0.2$–0.3; taking the lower values in each case gives

$$a_\mu(\text{weak}) = -28 \times 10^{-9} \tag{7.13}$$

for $\omega < 0$. The discrepancy between the new experimental value[30] for a_μ and the theoretical electromagnetic contributions[31] (through eighth order) is

$$\begin{aligned} a_\mu(\exp r) - a_\mu(em) &= [\,(1165\,922 \pm 9) \\ &\quad - (1165\,918 \pm 13)] \times 10^{-9} \\ &= (4 \pm 22) \times 10^{-9} \end{aligned} \tag{7.14}$$

which can be attributed to weak contributions. Allowing the two standard deviations, this is consistent with Eq. (7.13). The $g - 2$ restriction could be weakened by introducing other heavy leptons in the right-handed sector, e.g., the dominant $g_L g_R$ term in Eq. (7.11) would be eliminated if the right-hand doublet was $(M^{0\prime}, \mu^-)_R$ instead.

F. Further comments

The ω mixing provides an $E^- \to \nu_e$ coupling for the decay $E^- \to \nu_e(l^-\bar{\nu})$. The model can accommodate CP violation.[17] If only the left-handed sector Eq. (7.3) is retained, the model is natural in the sense of Ref. 32, $\bar{\nu}N$ anomalies may partially originate in the $u_L \to b_L$ coupling induced by ω mixing, atomic-physics parity violation must exist, and $\sigma(\nu_\mu e^-) \neq \sigma(\bar{\nu}_\mu e^-)$.

VIII. SUMMARY

The properties of neutrino trimuon events indicate heavy-lepton production with cascade decays. We have proposed a specific SU(2) × U(1) gauge model, which allows cascade lepton decays, and have made detailed calculations of the complete heavy-lepton production and decay chain. The model is in broad agreement with all trimuon distributions. We draw particular attention to the following results.

(i) The azimuth-momentum correlations of the data exclude a hadron-vertex mechanism for the extra muons in trimuon events and in some dimuon events.

(ii) The invariant-mass and transverse-momentum distributions of trimuon events indicate a mass of about 7 GeV for the primary heavy lepton M^-. The mass of the secondary heavy lepton M^0 is in the range 2–4 GeV.

(iii) A characteristic feature is the presence of two unobserved neutrinos, carrying off about 55% of the $\mu^-\mu^-\mu^+$ energy (about 35% of the total visible energy): this prediction can be tested in narrow-band beams.

(iv) The initial $\nu_\mu \to M^-$ coupling is necessarily $V - A$. The analysis is not especially sensitive to the $V \pm A$ nature of the other heavy-lepton couplings.

(v) Our cascade model predicts $\mu^-\mu^-$ events at about five times the trimuon rate, which is consistent with the present level of the data.

(vi) We predict $\mu^-\mu^+$ events from cascade decays, coming dominantly through the $M^0 \to \mu^-\mu^+\nu$ subchannel. The rate for $\mu^-\mu^+$ of heavy-lepton cascade decay origin is comparable to the $\mu^-\mu^-$ rate.

(vii) Heavy-lepton M^- production by ν_μ requires $\mu_L^- - M_L^-$ mixing. The observed cross section may require a mixing angle comparable to the Cabibbo angle, which would somewhat strain the limits of conventional μ-e universality. However, our ω-mixing scheme allows one to circumvent the conventional universality constraint and achieve a large $\nu_\mu \to M^-$ coupling, if required by future data.

*Work supported in part by the University of Wisconsin Research Committee with funds granted by the Wisconsin Alumni Research Foundation, and in part by the U. S. Energy Research and Development Administration under Contract No. E(11-1)-881, COO-596.

†On leave at the University of Wisconsin, supported by the Commission of Cultural Interchange between Spain and U. S. A.

‡On leave at the University of Wisconsin.

[1]M. Perl *et al.*, Phys. Rev. Lett. 35, 1489 (1975); Phys. Lett. 63B, 466 (1976); G. J. Feldman *et al.*, Phys. Rev. Lett. 38, 117 (1977).

[2]R. Felst, Bull. Am. Phys. Soc. 22, 20 (1977); H. Meyer, in Proceedings of the Coral Gables Conference, 1977 (unpublished).

[3]P. Baird *et al.*, Nature 264, 528 (1976).

[4]R. Barnett, Phys. Rev. D 13, 671 (1976); V. Barger, T. Weiler, and R. J. N. Phillips, *ibid.* 14, 1276 (1976); S. Nandi, Phys. Lett. 64B, 81 (1976); C. Albright and R. Schrock, Phys. Rev. D 16, 575 (1977).

[5]T. P. Cheng and L. F. Li, Phys. Rev. Lett. 38, 381 (1977).

[6]V. Barger and D. V. Nanopoulos, Univ. of Wisconsin-Madison Report No. COO-583, 1977 (unpublished).

[7]S. L. Glashow, Harvard Report No. HUTP-77/A008 (unpublished) B. W. Lee *et al.*, Phys. Rev. Lett. 38, 937 (1977); 38, 1230 (E) (1977); D. Horn and G. G. Ross, Phys. Lett. 67B, 460 (1977); J. E. Kim, Brown University report, 1977 (unpublished).

[8]A. Benvenuti *et al.*, Phys. Rev. Lett. 39, 1110 (1977); 39, 1183 (1977).

[9]B. C. Barish *et al.*, Phys. Rev. Lett. 38, 577 (1977).

[10]V. Barger, T. Gottschalk, and R. J. N. Phillips (unpublished); Phys. Rev. D 16, 746 (1977); Univ. of Wisconsin-Madison Report No. COO-603, 1977 (unpublished).

[11]S. L. Glashow, J. Iliopoulos, and L. Maiani, Phys. Rev. D 2, 1285 (1970).

[12]V. Barger and D. V. Nanopoulos, Nucl. Phys. B124, 426 (1977).

[13]P. Fayet, Nucl. Phys. B78, 14 (1974); J. D. Bjorken, K. Lane, and S. Weinberg, Phys. Rev. D 16, 1474 (1977).

[14]V. Barger, D. V. Nanopoulos, and R. J. N. Phillips, Univ. of Wisconsin-Madison Report No. COO-597, 1977 (unpublished).

[15]R. E. Marshak, Riazuddin, and C. P. Ryan, *Theory of Weak Interactions* (Wiley, New York, 1969).

[16]L. N. Chang, E. Derman, and J. N. Ng. Phys. Rev. D 12, 3539 (1975); C. H. Albright, *ibid.* 12, 1319 (1975); 13, 2508 (1976); A. Soni, *ibid.* 9, 2029 (1975); 11, 624 (1975).

[17]M. Kobayashi and K. Maskawa, Prog. Theor. Phys. 49, 652 (1973); J. Ellis, M. K. Gaillard, and D. V. Nanopoulos, Nucl. Phys. B109, 213 (1976); L. Maiani, Phys. Lett. 62B, 183 (1976); S. Pakvasa and H. Sugawara, Phys. Rev. D 14, 305 (1976); B. W. Lee, *ibid.* 15, 3394 (1977).

[18]V. Barger, T. Weiler, and R. J. N. Phillips, Nucl. Phys. B102, 439 (1976).

[19]A. Pais and S. B. Treiman, Phys. Rev. Lett. 35, 1206 (1975); A. Soni, Stony Brook Report No. ITP-SB-75-45 (unpublished); L. Baulieu, Nucl. Phys. B122, 100 (1977).

[20]V. Barger and R. J. N. Phillips, Phys. Rev. D 14, 80 (1976).

[21]C. H. Albright, J. Smith, and J. A. M. Vermaseren, Phys. Rev. Lett. 38, 1187 (1977).

[22]L. M. Sehgal and P. Zerwas, Nucl. Phys. B108, 483 (1976).

[23]A. Benvenuti *et al.*, Phys. Rev. Lett. 34, 419 (1975); 35, 1199 (1975); 35, 1203 (1975); 35, 1249 (1975).

[24]B. Barish *et al.*, Phys. Rev. Lett. 36, 939 (1976).

[25]M. Suzuki, Phys. Rev. Lett. 35, 1553 (1975); F. Gursey, P. Ramond, and P. Sikivie, Phys. Rev. D 12, 2166 (1975); Y. Abe *et al.*, Phys. Lett. 62B, 207 (1976); V. K. Cung and C. W. Kim, Phys. Rev. D 14, 1376 (1976).

[26]M. Perl, SLAC Report No. SLAC-PUB 1923, 1977 (unpublished).

[27]V. Barger, T. Gottschalk, D. V. Nanopoulos, and R. J. N. Phillips, Univ. of Wisconsin-Madison Report No. COO-598, 1977 (unpublished).

[28]S. Weinberg, Phys. Rev. D 5, 1412 (1972); A. Salam, in *Elementary Particle Theory: Relativistic Groups and Analyticity (Nobel Symposium No. 8)* (Almqvist and Wiksell, Stockholm, 1968), p. 367.

[29]See for example, E. S. Abers and B. W. Lee, Phys. Rep. 9C, 1 (1973).

[30]J. Bailey *et al.*, Phys. Lett. 67B, 225 (1977).

[31]J. Calmet *et al.*, Rev. Mod. Phys. 49, 21 (1977).

[32]S. L. Glashow and S. Weinberg, Phys. Rev. D 15, 1958 (1977); E. Paschos, *ibid.* 15, 1966 (1977); F. E. Paige, E. Paschos, and T. L. Trueman, *ibid.* 15, 3416 (1977).